



# Comprehensive outside Heat Transfer Coefficients by the use of End barrier warmth dimensions

## ABSTRACT

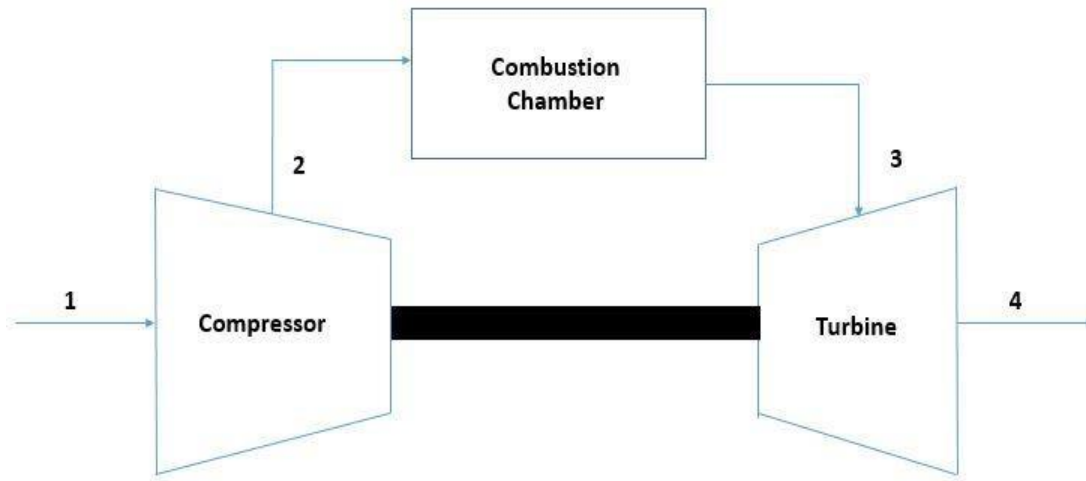
Short pins are used for internal cooling of the trailing edge in a gas turbine blade. A novel method is described in this thesis which helps in simplifying the experimental process used to obtain average heat transfer data on the pin surface, at the expense of additional post-processing complexity. The method is based on a unique, analytical solution of the longitudinal conduction equation with internal heat generation, allowing computation of heat transfer rates via pin base temperature measurements via Temperature Sensitive Paint, or similar non-intrusive methods. Verification of this method is done with comparisons to the solution of infinite fins with internal heat generation, conjugate computational results, and experimental data validated against the literature. Agreement within 8% of experimental and 2% of numerical results confirm the suitability of the method.

**Keywords** – Average heat transfer coefficient ,CFD ,internal heat generation,non intrusive method

## 1. Introduction

### Motivation-The Need for Gas Turbine Cooling

Most passenger aircrafts operating today are powered by gas turbine engines. Gas turbine engines are preferred for flight due to their high power-to-weight ratio as well as their robustness and efficiency in delivering power. High power output at maximum efficiency is one of the major requirements for engine manufacturers and designers as this helps in reducing fuel usage and ultimately operating costs for airlines. The Brayton cycle describes the working of a gas turbine engine as shown in Fig



ideal Brayton cycle consists of adiabatic compression in the compressor section(1-2), constant pressure heat addition in the combustor (2-3) and the last step in the process, expansion for energy extraction in the turbine section (3-4). The energy obtained from the turbine drives the compressor in this process. In simpler words, freestream air is

compressed in the compressor section and introduced in the combustor where fuel is added to this compressed air and ignited. This mixture of hot gas is then introduced into the turbine section where the turbine blades extract energy.

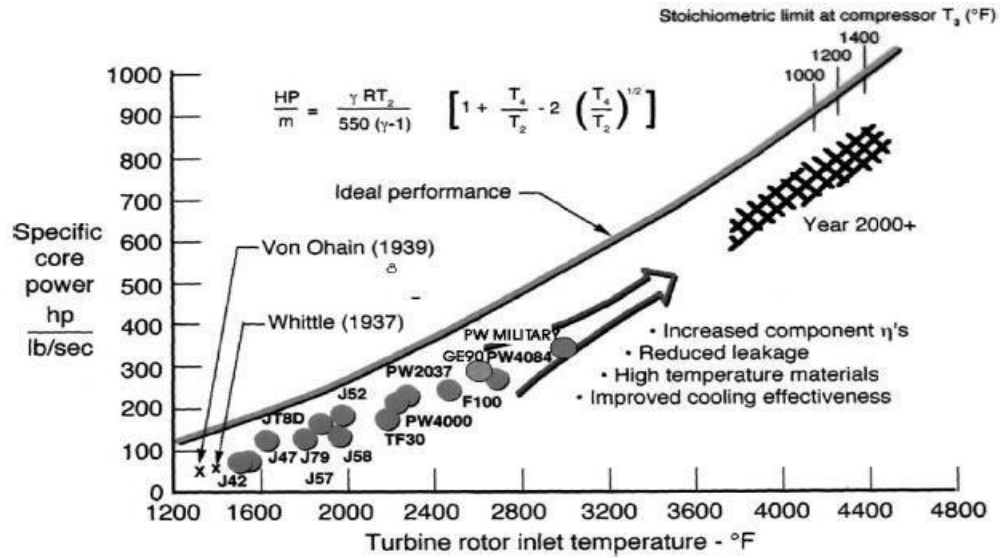
The isentropic efficiency of a gas turbine engine is given by:

$$\eta = 1 - \frac{T_4}{T_3}$$

where  $T_3$  = Turbine Inlet Temperature  $T_4$  = Turbine Exit Temperature

Thus, from the above equation we can see that an increase in turbine inlet temperature results in an increase in the efficiency of a gas turbine engine. Figure 1-2 shows the increase in engine power for various engines with a corresponding increase in turbine inlet temperature.

## Fundamentals of Heat Transfer & Extended Surfaces



Before we delve into the different types of methods used in gas turbine cooling, we must try and understand the fundamentals of heat transfer and cooling. There are three primary modes of heat transfer; conduction, convection & radiation. The first two modes are discussed in detail here since the focus of this thesis primarily deals with these.

Conduction may be viewed as the transfer of energy from the more energetic to the less energetic particles of a substance due to interactions between the particles. In simpler words, it can be defined as the transfer of heat between the hot surface and the colder surface, which are in physical contact with each other, because of the existing temperature gradient between them. The rate of conduction heat transfer is given by Fourier's Law:

## 2 Literature Review

A significant amount of studies have been conducted with regards to pin-fin cooling at the trailing edge of the turbine; experimentally as well as computationally. Some of the earliest works included trying to correlate the heat transfer characteristics between long tubes in cross flow heat exchangers and very short pins in plate-fin heat exchangers with pin-fin channels in a turbine blade. The difference between the three cases being in the height to diameter ratio (H/D). The pin-fins in an internal cooling channel of a gas turbine blade have a H/D ratio between the other two applications. Armstrong and Winstanley(1988) found that the interpolation between the two extreme cases did not accurately predict the performance characteristics of pin-fins in a gas turbine blade. The effect of conducting and non-conducting array of pins on surface average Nusselt number was studied by Metzger & Haley (1982, 1984) and by VanFossen (1982). Investigations were also done to obtain correlations for staggered and inline arrays by a host of researchers. (Sparrow (1980,2004),

VanFossen (1982), Metzger et al., (1982), Chyu(1998)). Alternative pin geometries were compared against the baseline circular cylindrical pins for their pressure loss benefits by Goldstein et al., (1994), Chyu (1996, 1998) and Camci et al., (2005). Pin and row removal studies were also conducted to investigate the pressure loss and heat transfer characteristics by Sparrow & Molki (1982) and recently by Kirsch et al. (2014). As the focus of research areas in regards to pin-fin cooling changed over the years, so did the experimental measurement techniques. In the 1980's, thermocouples were the preferred method of acquiring temperature data (Metzger & Haley (1982), VanFossen (1982, 1984) Sparrow (1980)). In the 1990's, heat transfer characteristics of the pin surface were studied via a mass transfer analogy using a naphthalene sublimation technique (Goldstein et al., (1994), Chyu (1998,1999), Sparrow (1984)). In the late 90's and 2000's, non-intrusive techniques such as IR and TLC were used to acquire endwall and pin surface data (Camci et al. (2005), Ames et al., (2007), Lawson et al. (2011), Kirsch et al., (2013)). Some of these studies are reviewed in detail in the following section.

VanFossen (1981, 1984) investigated the effects of pin height and pin inclination in a pin fin array. For his experiments, he utilized a staggered array of 4 rows but used two different set of pins. The first set of pins had an  $H/D = 0.5$  and  $X/D = 2$  while the configuration of the other set of pins was twice of this. Two separate arrays consisting of wooden and copper pin arrays were used to isolate and study the contribution of endwall and the pin surface individually. Only the endwalls were heated and maintained at a constant temperature. Thermocouples were used to obtain temperature data. He found that heat transfer coefficients on the pin surface were about 35% higher than the endwall. Inclined pins were found to have the same heat transfer characteristics as compared to the pins that are perpendicular to the endwall. Another study conducted by Brigham and VanFossen (1984) concluded that short pin fins indicated lower levels of heat transfer compared to longer pins of same design and that heat transfer augmentation is strongly dependent on the  $H/D$  ratio.

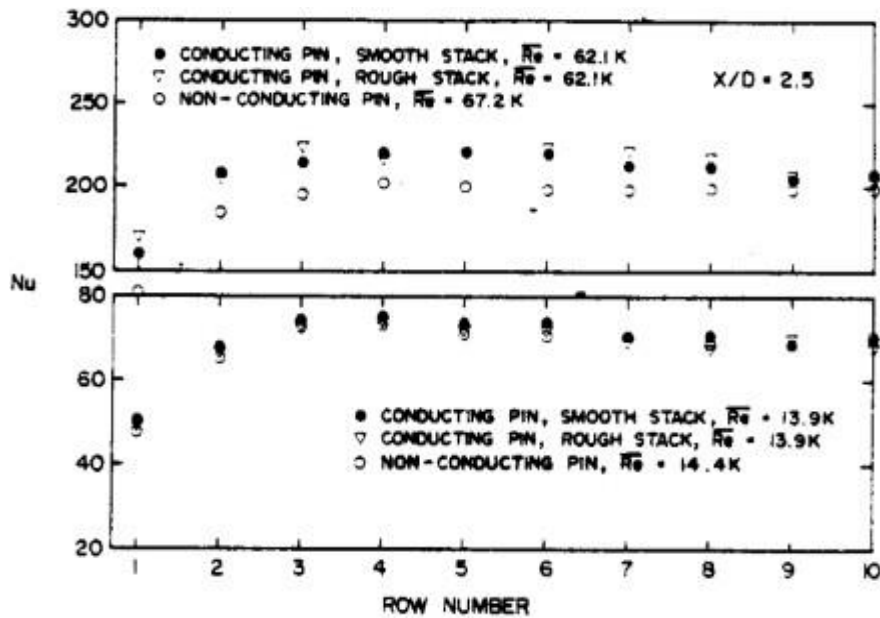
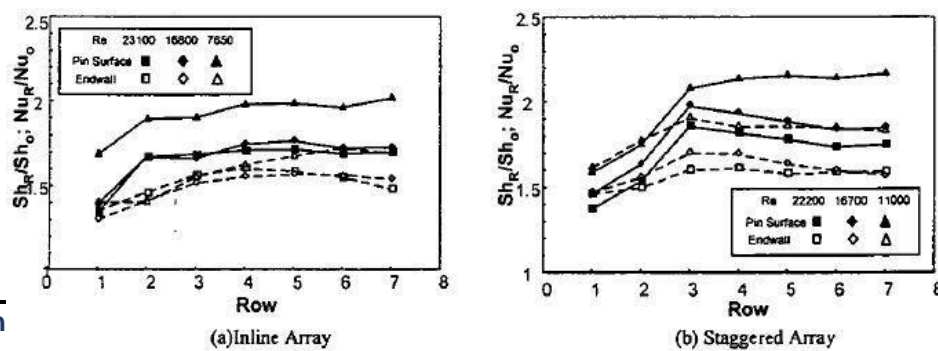


Figure 2-1. Row averaged Nu for conducting and non-conducting pin arrays. (Metzger & Haley, 1982)

Since this was a study to obtain row averaged Nusselt number, thermocouples were used at each row to obtain temperature data. Additional thermocouples were attached to account for failure. For each array configuration, pin type and flow rate, 2 power levels were used, corresponding to segment temperatures approximately  $6^{\circ}C$  and  $12^{\circ}C$  above the duct flow bulk temperature. Figure 2-1 shows that the difference in Nusselt number between conducting and non-conducting pins is negligible for the low Reynolds number case. Similar to many other researchers, they observed heat transfer augmentation up to row 3 and then a periodically fully-developed rate of augmentation till the last row.

Chyu et al., (1990, 1999) used a naphthalene sublimation technique to study the individual heat transfer contributions from the pin as well as endwall using a mass transfer analogy. This setup helped them to ensure that the entire wetted surface in a pin fin channel was thermally active. He also noted that the variety of thermal boundary modelling used by researchers for a pin-fin array did not influence the general trends of heat transfer as significantly as the individual magnitudes due to bulk flow temperature variations.

The mass transfer co-efficient or the Sherwood number is analogous to the Nusselt number in heat



transfer. Chyu (1999) used aluminum pins and investigated both inline and staggered arrays for Reynold's numbers of 7650, 16800 & 23100. A constant wall temperature boundary condition was utilized at the endwall. Figure 2-2 shows the row averaged Sherwood numbers at the pin surface and endwall for different Reynold's numbers. As we can see from Fig. 2-2, he concluded that the heat transfer coefficient on the pin surface is higher than that on the uncovered end wall by approximately 10-20% as compared to 30-40% obtained by VanFossen(1982)

### 3 Problem Statement

As we saw in the previous section, researchers have been using different thermal boundary conditions when studying the thermal performance of pin-fin arrays. Since the flow in an internal cooling channel of a gas turbine blade is turbulent, the heat transfer characteristics are highly dependent on the fluid properties i.e. Reynold's number and Prandtl number and show very weak dependency on the thermal boundary condition (Bejan, 2003). Each boundary condition arrangement has corresponding advantages as well as ensuing complexity in the experimental setup. The reason for using different thermal boundary conditions is to simplify the complicated experimental setup and as well as to compensate for manufacturing limitations. In most of the experiments, either the pin is heated or the endwall.

Since the flow-field in a pin-fin cooling channel is highly complex and non- uniform, many thermocouples would need to be attached to obtain data from the entire testsurface. The use of thermocouples is accompanied by additional machining of holes on the pin and endwalls. Often, additional thermocouples are attached in the event of failure of the original thermocouple. Thus, for a pin-fin array, use of thermocouples is accompanied by large setting up times due to the additional machining that is required. Internal heat generation within the pin is required to maintain a sufficient temperature difference between the pin surface and coolant, reducing experimental uncertainty.

Thus, certain simplifications can be made either on the experimental side or the post-processing side for the ease and shorter turn-around times of testing. Validation tests need to be done with well-established experiments. In terms of the design process, experimental verification is the step following the elimination of the initial geometries

through numerical simulations. As we can see, there is a need for predicting average heat transfer coefficients on the surface of a fin through non-intrusive techniques to reduce the turnaround times associated with experimental setup.

The hypothesis of this study is that the base temperature of the pin can be used to obtain accurate pin surface average heat transfer coefficients. The new method prescribed in this thesis aims to simplify the setting up process at the cost of additional post-processing complexity.

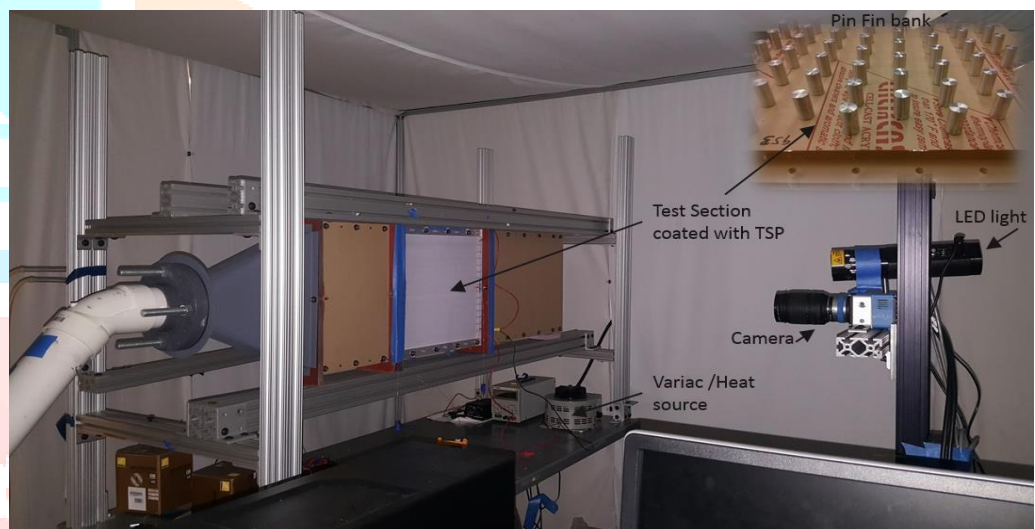
## Methodology

### Experimental Setup

The test section, shown in Figure 4-1, is manufactured from 2.54cm (1") thick optically clear acrylic. Figure 4-1 also shows the sCMOS camera used for recording TSP emission, the TSP excitation LED lights along with the current source. The working of TSP is detailed in the next section. Acrylic was chosen as it allows suitable optical access for TSP measurements, as well as its insulation properties. The current pin-fin array consists of 8 rows, having 7 full cylindrical, aluminum pins in each row arranged in a staggered manner. The arrangement for this study was also used for previous investigations by Fernandes (2015) and Prasad (2016).

Figure 4-1. Experimental Setup.

Figure 4-2 shows the schematic of the flow loop used for the experiments. The centrifugal blower was operated in suction mode for all experiments. The flow was controlled using gate valves. The venture flow



meter gave the difference in pressure

between the flow upstream and downstream which was used to determine the mass flowrate and ultimately the average velocity of flow in the channel.

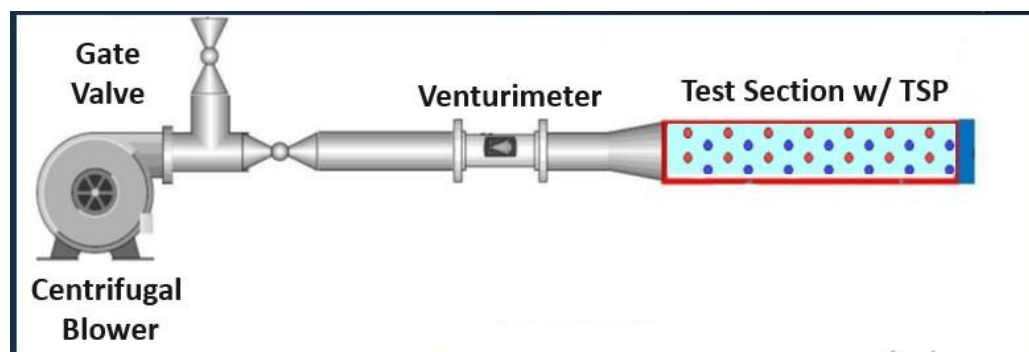


Figure 4-3 shows the non-dimensional distances in the channel. Taking the pin diameter as the reference diameter, the non-dimensional streamwise ( $X/D$ ) and spanwise distance ( $Y/D$ ) between the pins was

chosen to be 3 based on previous research (Ames et al., (2006), Metzger & Haley (1982), VanFossen (1982)).

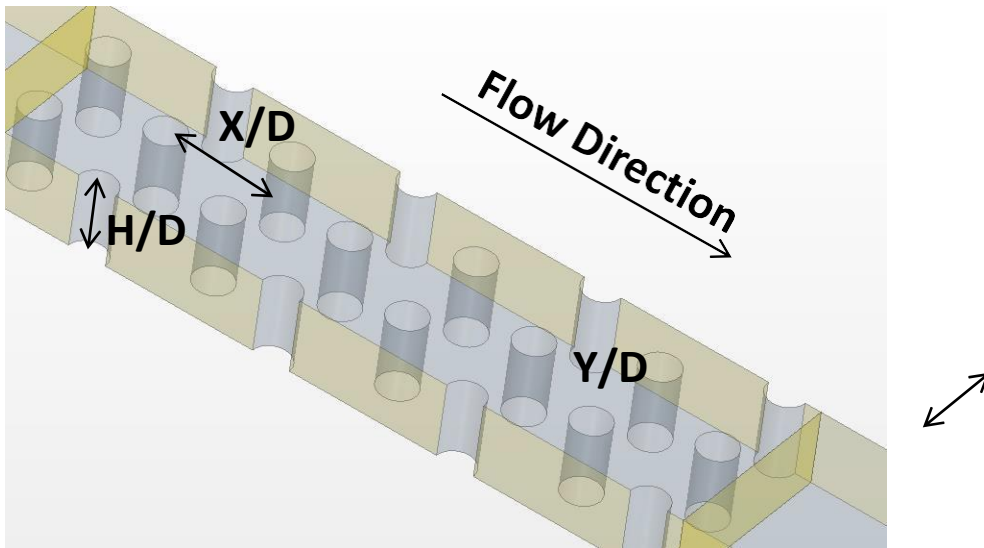
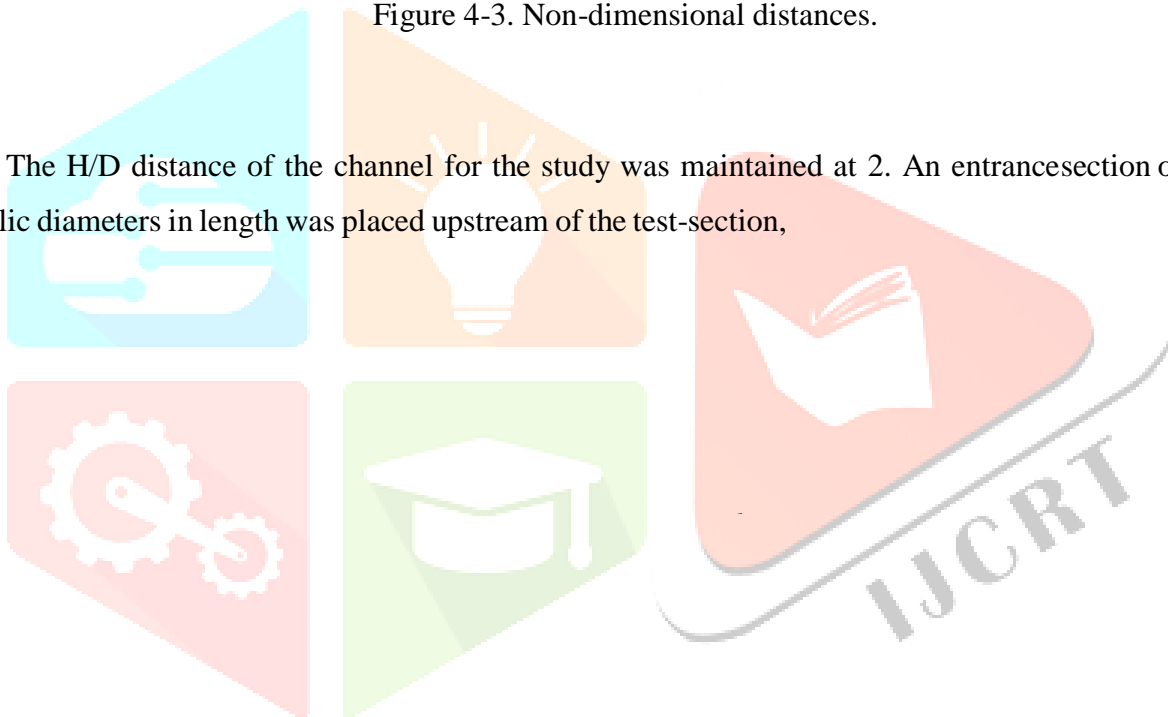


Figure 4-3. Non-dimensional distances.

The  $H/D$  distance of the channel for the study was maintained at 2. An entrance section of 10 channel hydraulic diameters in length was placed upstream of the test-section,





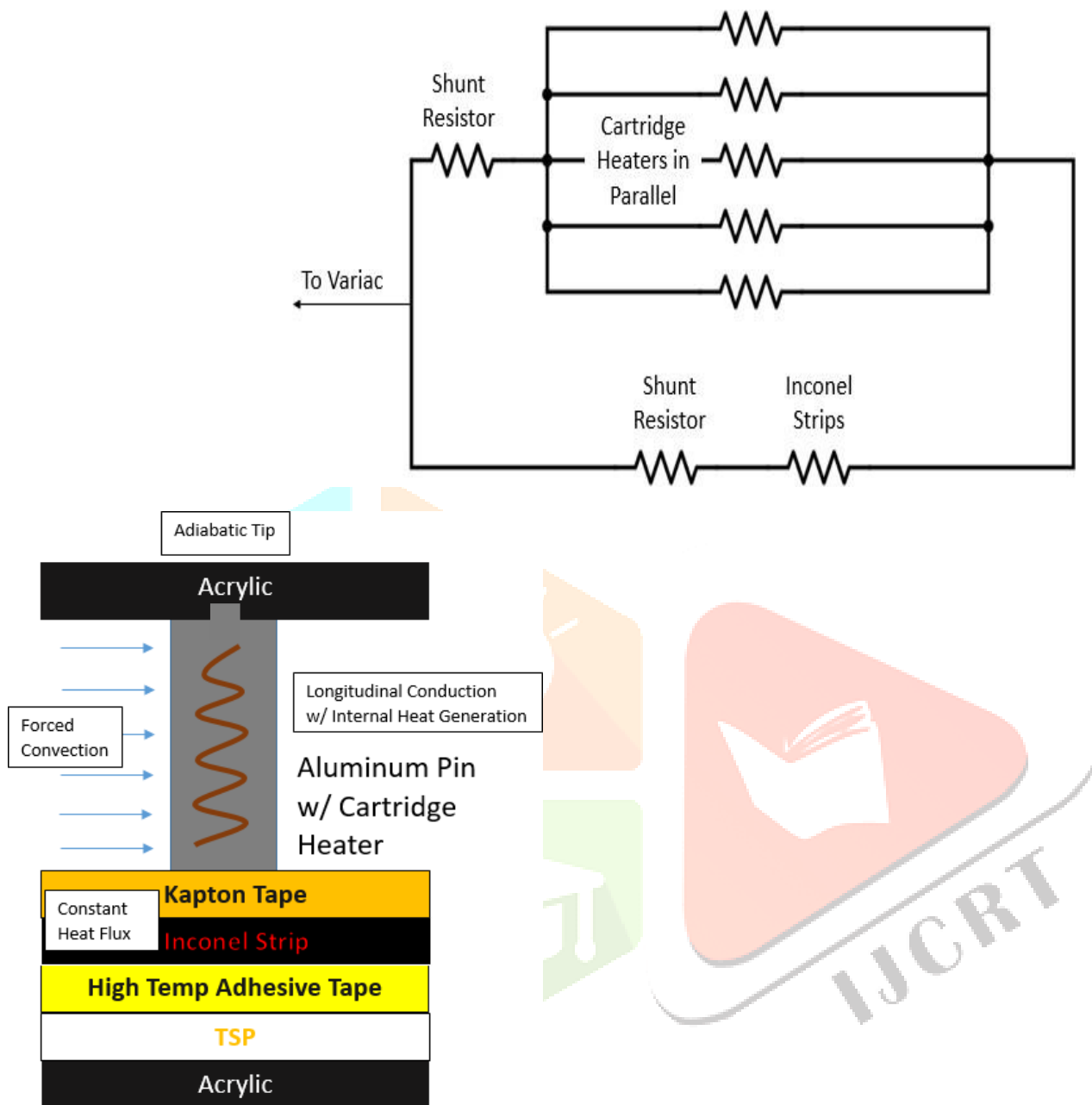
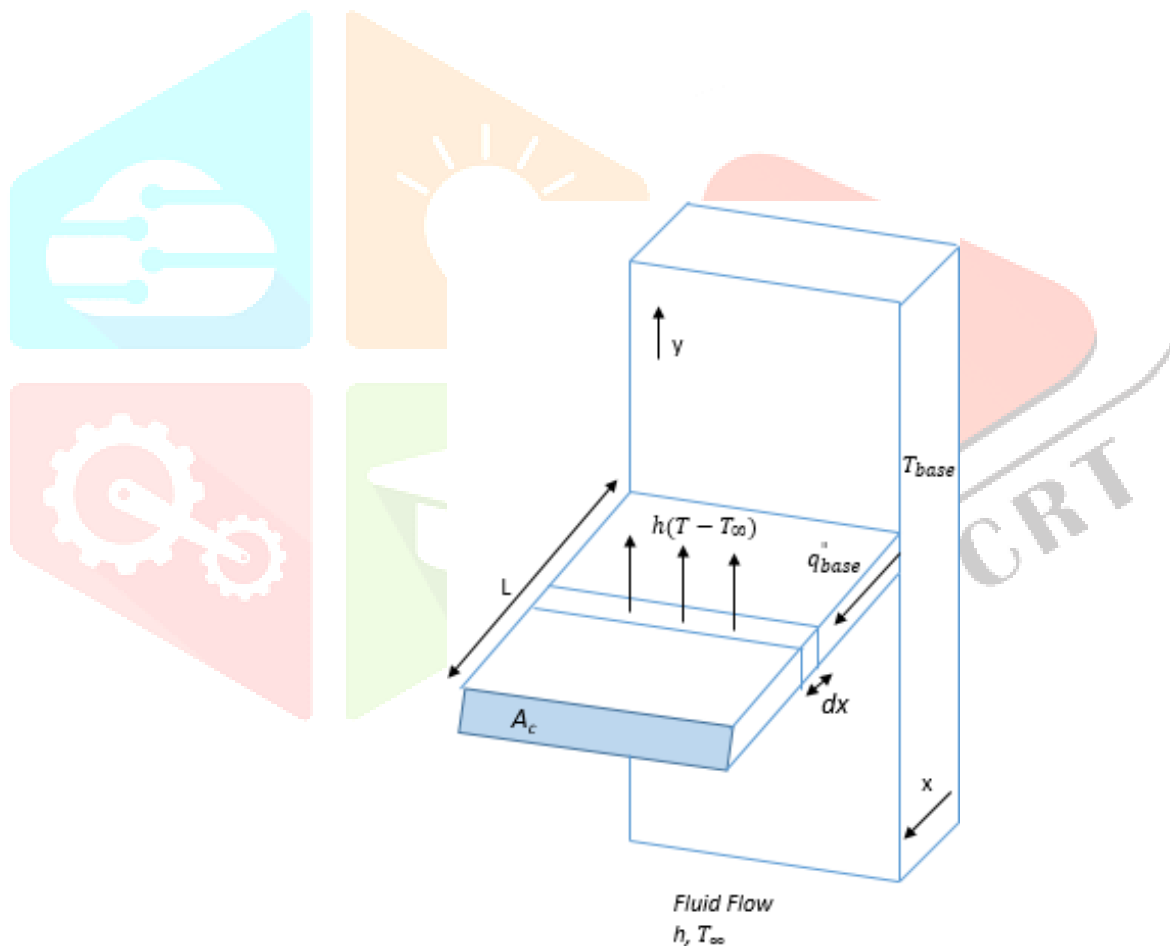


Figure 4-6. Circuit Diagram of the entire setup

## 2. Extended Surface Methodology (ESM)

### Introduction to Extended Surface Analysis

One of the easiest and powerful methods for simplification of analysis for a pin-fin channel is the 1-D analytical model based on the extended surface theory. Using this, we can predict the surface average heat transfer coefficients on the extended surface. Figure 5-1 shows the simplest model of an extended surface of finite length  $L$ , cross-sectional area  $A_c$ , thermal conductivity  $k$  and perimeter  $P$ . The extended surface is in physical contact with a hot surface at temperature,  $T_{base}$ . Surrounding the extended surface is a fluid having heat transfer coefficient  $h$ , at temperature  $T_\infty$  such that  $T_{base} > T_\infty$ .



Tip Condition	Temperature distribution $\frac{\theta}{\theta_{base}}$	Fin Heat Transfer $q_{base}$
Convective heat transfer $h\theta(L) = -k \left( \frac{d\theta}{dx} \right)_{x=L}$	$\frac{\cosh m(L-x) + \frac{h}{mk} \sinh m(L-x)}{\cosh mL + \frac{h}{mk} \sinh mL}$	$M \frac{\cosh m(L-x) + \frac{h}{mk} \sinh m(L-x)}{\cosh mL + \frac{h}{mk} \sinh mL}$
Adiabatic Tip $\left( \frac{d\theta}{dx} \right)_{x=L} = 0$	$\frac{\cosh m(L-x)}{\cosh mL}$	$M \tanh mL$
Given temperature $\theta(L) = \text{Known}$	$\frac{\frac{\theta_L}{\theta_{base}} \sinh m(L-x) + \sinh mL}{\sinh mL}$	$M \frac{\cosh mL - \frac{\theta_L}{\theta_{base}}}{\sinh mL}$
Infinitely long fin $\theta(L) = 0$	$e^{-mx}$	$M$

## 6 Results & Discussion

### Analytical Verification Results

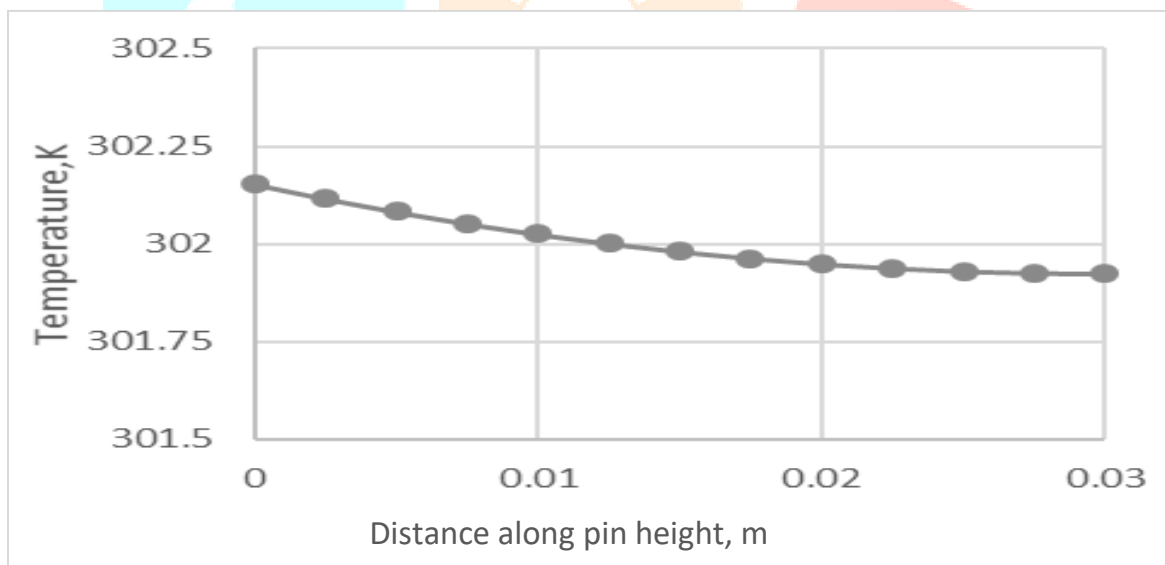
To verify the analytical solution obtained in section 5.2, it was compared to the standard solution presented in heat transfer handbooks for a fin of infinite length with similar boundary conditions. (Bejan, 2003) The solution for a fin of infinite length with constant heat flux at the base is given by equation (18).

However, it should be noted that equation (18) is a solution for a pin of infinite length and hence to compare with equation (21), the current model was implemented with the condition  $mL \geq 4.2$  Table 1 lists the parameters used for the comparison between the two solutions. These parameters are representative of our experimental setup.

Using the parameters listed in Table 6-1, taking the infinite length to be 0.3m, we observe that our analytical solution matches that of Bejan's exactly, as shown in Figure 6-1.

Table 6-1. Pin parameters

Pin diameter (D)	0.015 m
Actual Pin height	0.03 m
Infinite Fin Approximation height (L)	0.3 m
$h$	200 W/m <sup>2</sup> -K
$k$ (aluminum)	205 W/m-K
$T_{\infty}$	300 K
$q_b''$	3200 W/m <sup>2</sup>
$Bi$	0.00297
$\dot{q}$	3.116 W/m <sup>3</sup>



## Computational Verification Results

First, the pin surface average Nusselt number was obtained from the simulation. Second, the average base temperature of the pin as obtained from the simulation was input into the non-linear equation (21) and solved iteratively using MATLAB® to obtain the surface average heat transfer coefficient. This heat transfer coefficient was then non-dimensionalised as the Nusselt number and compared with the value obtained from the simulation. The initial guess for the non-linear equation was obtained from the theoretical fin parameter

based on previous experimentation i.e values in Table 1. It was found that the solution was not dependent on the initial guess for the non-linear equation since MATLAB® uses a Trust-region Dogleg method (MathWorks Documentation, MATLAB2015b, 2015). More information on this method can be found in the user document.

As we can see from Table 6-2, the pin surface averaged Nusselt number obtained from our analytical methodology is in close agreement with the value obtained via CFD.

### Rig Validation- Intensity of Lights

One of the earliest tests done to validate our experimental setup was the intensity of lights test. As mentioned earlier, temperatures are determined from TSP using the intensity ratio of the reference and data image. The accuracy of the intensity captured is dependent on the stability of the light intensity emitted by the light source, UV light in this case. Readings would be consistent only if there is minimal fluctuation of intensity. Hence, it is very important to know the time taken by the light to reach a stable intensity. The point of this test was to establish a suitable “warm-up” time for the UV lights to reduce uncertainty.

Figure 6-4 shows the intensity stabilization over time for one such test.

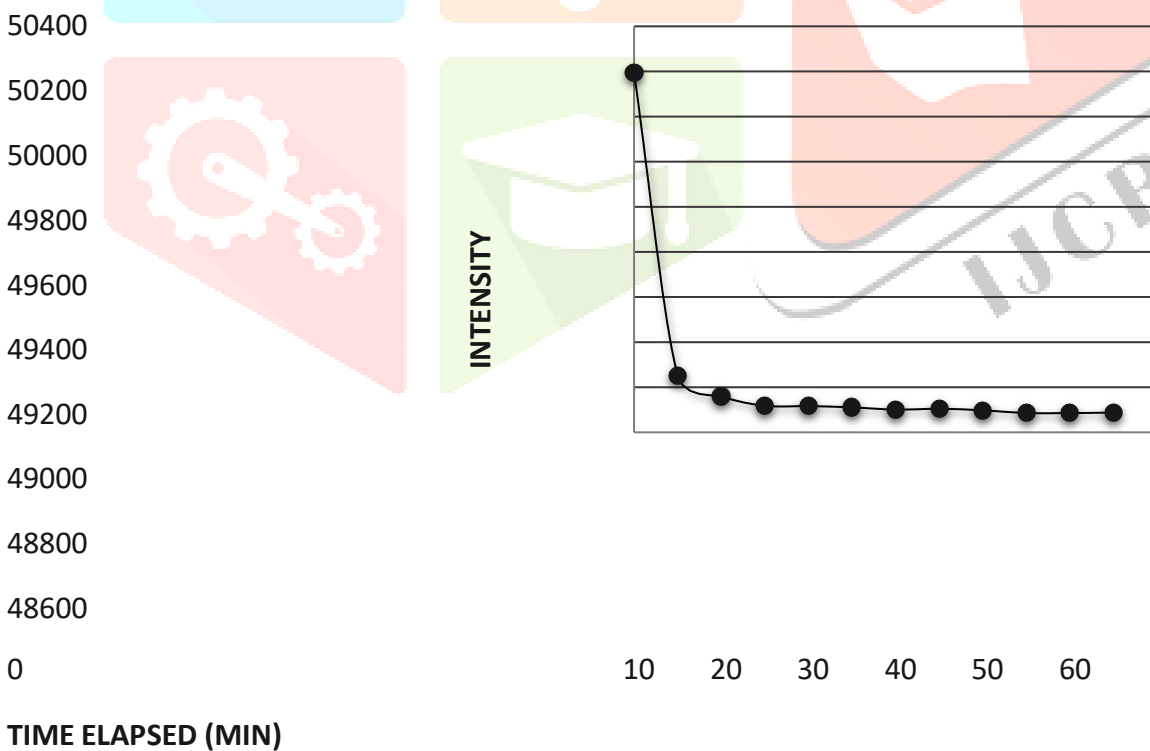
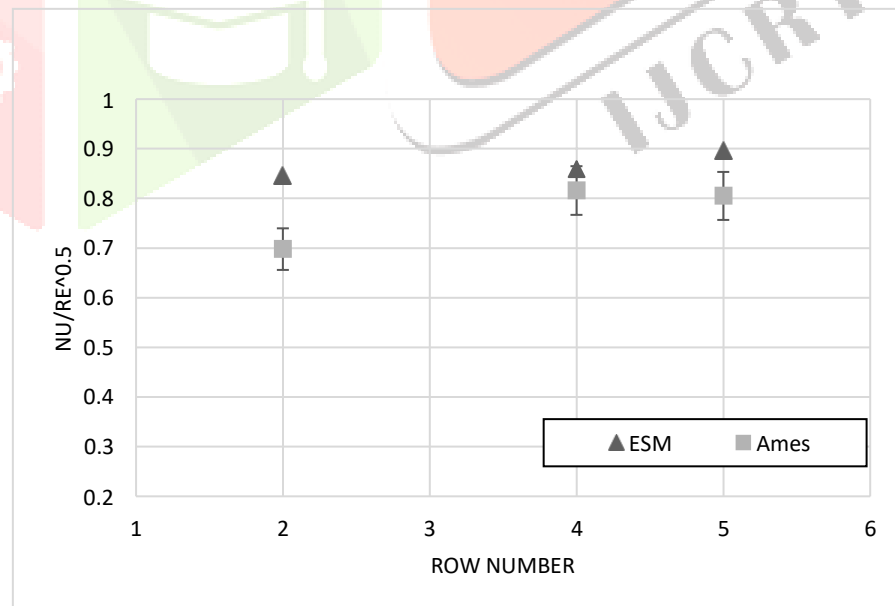


Figure 6-4. Intensity Stabilization over time

The UV light is shone upon a white paper such that it is uniformly illuminated. The

focal length and exposure time adjustments of the CMOS camera are made such that the maximum possible intensity is captured by it. Four images were captured & saved for a single time instance to average out the intensities. The overall time and the exposure time were recorded. Images were taken at 5 minute intervals. The tests were conducted for two different exposure times. As we can see from Figure 6-4, the intensity of lights stabilizes after 10 minutes and hence, the warm up time for the lights was established to be about 10 minutes.

As mentioned earlier, Ames et al. (2006) obtained midline circumferential distribution of Nusselt number for a single pin through rows 1-5 of a staggered pin-fin array in the form of  $Nu/Re^{0.5}$  for Reynolds numbers of 3,000, 10,000 and 30,000. This was accomplished by employing 24 thermocouples machined around the pin surface, equidistant from each other. This circumferential distribution was then averaged to obtain a single value of Nusselt number corresponding to each row and Reynolds number. Our experiment had cartridge heaters machined into individual pins of rows 2,4,5,7 & 8. Thus, comparison is done for pins of rows 2,4 and 5. Figure 6-8, 6-9 & 6-10 show the comparison between Ames' data and the analytical solution for the 3 cases.



## 7 conclusion

The purpose of this study was to provide a new methodology to obtain pin surface average heat transfer coefficients in pin fin cooling experimentation by using non-intrusive techniques such as TSP. This methodology was verified analytically, numerically as well as experimentally. The hypothesis was that the base temperature of the pin can be used to predict surface average heat transfer coefficients of the pins. The base temperature at the pin was determined using TSP. This helps in reducing setting up times and complexity of the experimentation at the cost of additional post processing efforts.

1. An analytical solution was obtained to do the same for the boundary conditions common to pin fin cooling experimentation as well as the in-house experimental rig. The analytical solution with a few minor modifications was verified after comparison with a standard solution listed in heat transfer reference books. The need for raising the pin surface temperature using internal heat generation via the use of cartridge heaters was also shown by the analytical solution.

2. A conceptual validation of the method using CFD was also undertaken. Two cases were run, first a conduction only case and second, a CHT case. Nusselt numbers obtained using this analytical method were found to be within 2% of the simulation results.

3. For experimental validation, a study conducted by Ames et al, was chosen for comparison. The reason being their experimental setup was similar to in house experimental setup. Pin surface average Nusselt numbers were compared for pins from

rows 2,4 & 5 for Reynold's numbers of 3,000, 10,000 & 30,000. The highest error on an average was found to be for row 2 for all Reynold's numbers of about 25%. This could be attributed to the fact that the in house experimental rig did not have a heated entrance length contrary to Ames' experiment. Nusselt numbers for row 4 and row 5 on an average, for all Reynold's numbers, showed an error of 8% and 12% respectively.

## 8 REFERENCES

Ames, F. E., Dvorak, L. A., & Morrow, M. J. (2004, January). Turbulent augmentation of internal convection over pins in staggered pin fin arrays. In *ASME Turbo Expo 2004: Power for Land, Sea, and Air* (pp. 787-796). American Society of Mechanical Engineers.

Ames, F. E., & Dvorak, L. A. (2006, January). The influence of Reynolds number and row position on surface pressure distributions in staggered pin fin arrays. In *ASME Turbo Expo 2006: Power for Land, Sea, and Air* (pp. 149-159). American Society of Mechanical Engineers.

Ames, F. E., & Dvorak, L. A. (2006). Turbulent transport in pin fin arrays: experimental data and predictions. *Journal of turbomachinery*, 128(1), 71-81.

Ames FE, Nordquist CA, Klennert LA. Endwall Heat Transfer Measurements in a Staggered Pin Fin Array With an Adiabatic Pin. ASME. Turbo Expo: Power for Land, Sea, and Air, Volume 4: Turbo Expo 2007, Parts A and B ():423-432. doi:10.1115/GT2007-27432

Armstrong JJ, Winstanley DD. A Review of Staggered Array Pin Fin Heat Transfer for Turbine Cooling Applications. ASME. J. Turbomach. 1988;110(1):94-103. doi:10.1115/1.3262173.

Baughn JW, Ireland PT, Jones TV, Saniei NN. A Comparison of the Transient and Heated-Coating Methods for the Measurement of Local Heat Transfer Coefficients on a Pin Fin. ASME. Turbo Expo: Power for Land, Sea, and Air, Volume 4: Heat Transfer; Electric Power; Industrial and Cogeneration ():V004T09A031. doi:10.1115/88-GT-180.

Bejan, A., & Kraus, A. D. (2003). Heat transfer handbook (Vol. 1). John Wiley & Sons. Bell, James, Schairer, E., Hand, L., Mehta, R. (2001). "Surface Pressure Measurements Using Luminescent Coatings". *Journal of Fluid Mechanics*, 33, pp 155-206.

Bernard L. Koff, "Gas Turbine Technology Evolution: A Designer's Perspective", Turbo Vision, Inc., Palm Beach Gardens, Florida, 2004.

Brigham, B. A., & Van Fossen, G. J. (1984). Length to diameter ratio and row number effects in short pin fin heat transfer. *ASME, Transactions, Journal of Engineering for Gas Turbines and Power (ISSN 0022-0825)*, 106, 241-245.

Boyce M. P. (2006), Gas Turbine Engineering Handbook, 3rd Edition.

Chang, S. W., Yang, T. L., Huang, C. C., & Chiang, K. F. (2008). Endwall heat transfer